



Silent plaque ruptures in non-obstructive lesions of non-infarct-related arteries: a multimodality, serial intracoronary imaging study

Ryota Kakizaki ¹, Flavio G. Biccirè^{1,2,3}, Sylvain Losdat⁴, Yasushi Ueki⁵, Jonas D. Häner¹, Hiroki Shibutani⁶, Tatsuhiko Otsuka⁷, Sarah Bär¹, Jacob Lønborg ⁸, Ernest Spitzer ^{9,10}, George C.M. Siontis¹, Anna S. Ondracek¹¹, Robert-Jan van Geuns ¹², Yu-Jen Wang ¹³, Christian M. Matter^{13,14}, Juan F. Iglesias¹⁵, David Spirk ¹⁶, Joost Daemen ¹⁷, Gregor Fahrni^{18,19}, Felix Mahfoud^{20,21}, Thomas Engstrøm ⁸, Irene M. Lang¹¹, Konstantinos C. Koskinas¹, and Lorenz Räber ^{1,*}

¹Department of Cardiology, Bern University Hospital, Inselspital, University of Bern, Freiburgstrasse 18, Bern 3010, Switzerland; ²Department of Cardiovascular Sciences, San Giovanni Addolorata Hospital, Rome, Italy; ³Department of Cardiovascular Sciences, Sapienza University of Rome, Rome, Italy; ⁴Department of Clinical Research, University of Bern, Bern, Switzerland; ⁵Department of Cardiovascular Medicine, Shinshu University School of Medicine, Nagano, Japan; ⁶Division of Cardiology, Department of Medicine II, Kansai Medical University, Osaka, Japan; ⁷Department of Cardiology, Itabashi Chuo Medical Center, Tokyo, Japan; ⁸Department of Cardiology, Rigshospitalet, Copenhagen University Hospital, Copenhagen, Denmark; ⁹Cardialysis, Rotterdam, The Netherlands; ¹⁰Department of Cardiology, Thoraxcenter, Erasmus University Medical Center, Rotterdam, The Netherlands; ¹¹Department of Cardiology, Medical University of Vienna, Vienna, Austria; ¹²Department of Cardiology, Radboud UMC, Nijmegen, The Netherlands; ¹³Center for Translational and Experimental Cardiology (CTEC), Department of Cardiology, University Hospital Zurich and University of Zurich, Zurich, Switzerland; ¹⁴Department of Cardiology, University Heart Center, University Hospital Zurich, Zurich, Switzerland; ¹⁵Department of Cardiology, Geneva University Hospitals, Geneva, Switzerland; ¹⁶Institute of Pharmacology, Bern University Hospital, University of Bern, Bern, Switzerland; ¹⁷Department of Cardiology, Erasmus University Medical Center, Rotterdam, The Netherlands; ¹⁸Department of Cardiology, Stadtspital Zürich, Zürich, Switzerland; ¹⁹Department of Clinical Research, University of Basel, Basel, Switzerland; ²⁰Department of Cardiology, University Heart Center, University Hospital Basel, Basel, Switzerland; and ²¹Cardiovascular Research Institute Basel (CRIB), University Heart Center, University Hospital Basel, Basel, Switzerland

Received 20 July 2025; revised 10 October 2025; accepted 15 January 2026

Abstract

Background and Aims

Plaque rupture can occur at non-obstructive lesions in non-infarct-related coronary arteries (non-IRAs) without inducing ischaemia. This study aimed to: (1) assess the frequency and lesion characteristics of plaque rupture in non-IRAs of acute myocardial infarction (AMI) patients, (2) evaluate morphological changes in rupture sites over 52 weeks, and (3) investigate the baseline morphology of new-onset ruptures.

Methods

This study analysed pooled data from the IBIS-4 and PACMAN-AMI trials. Patients presenting with AMI underwent multimodality intracoronary imaging of non-IRAs at baseline and after 52 weeks.

Results

Among 783 lesions from 336 patients evaluated at baseline, plaque rupture was observed in 41 lesions of 40 patients (12%). Biomarkers including lipid and inflammation markers were comparable between patients with and without rupture in non-IRAs. Lesions with rupture showed larger percent atheroma volume (53.3 ± 6.4 vs. $49.5 \pm 5.8\%$, estimated difference $3.6[1.9$ to $5.4]$), larger external elastic membrane area (20.5 ± 4.8 vs. 15.7 ± 5.6 mm², $4.1[2.5$ to $5.7]$), and smaller minimum fibrous cap thickness (69 ± 49 vs. 116 ± 84 μm, $-43[-75$ to $-11]$) compared to those without. Among 41 rupture sites assessed serially, 21 (51%) healed by

* Corresponding author. Tel: +41 31 632 50 00, Email: lorenz.raeber@insel.ch

The institution where the work was performed: Bern University Hospital Inselspital, Bern, Switzerland

© The Author(s) 2026. Published by Oxford University Press on behalf of the European Society of Cardiology. All rights reserved. For commercial re-use, please contact reprints@oup.com for reprints and translation rights for reprints. All other permissions can be obtained through our RightsLink service via the Permissions link on the article page on our site—for further information please contact journals.permissions@oup.com.

52 weeks. At follow-up, 10 rupture sites were newly identified, and thin-cap fibroatheroma was the most frequent baseline morphology of those.

Conclusions

Plaque rupture in non-obstructive lesions of non-IRAs was present in 12% of AMI patients. Larger plaque volume, positive remodeling, and thinner fibrous cap were associated with rupture. More than half of untreated ruptures transitioned into stable morphologies. Thin-cap fibroatheroma was the most frequent underlying morphology of new-onset rupture.

Structured Graphical Abstract

Key Question

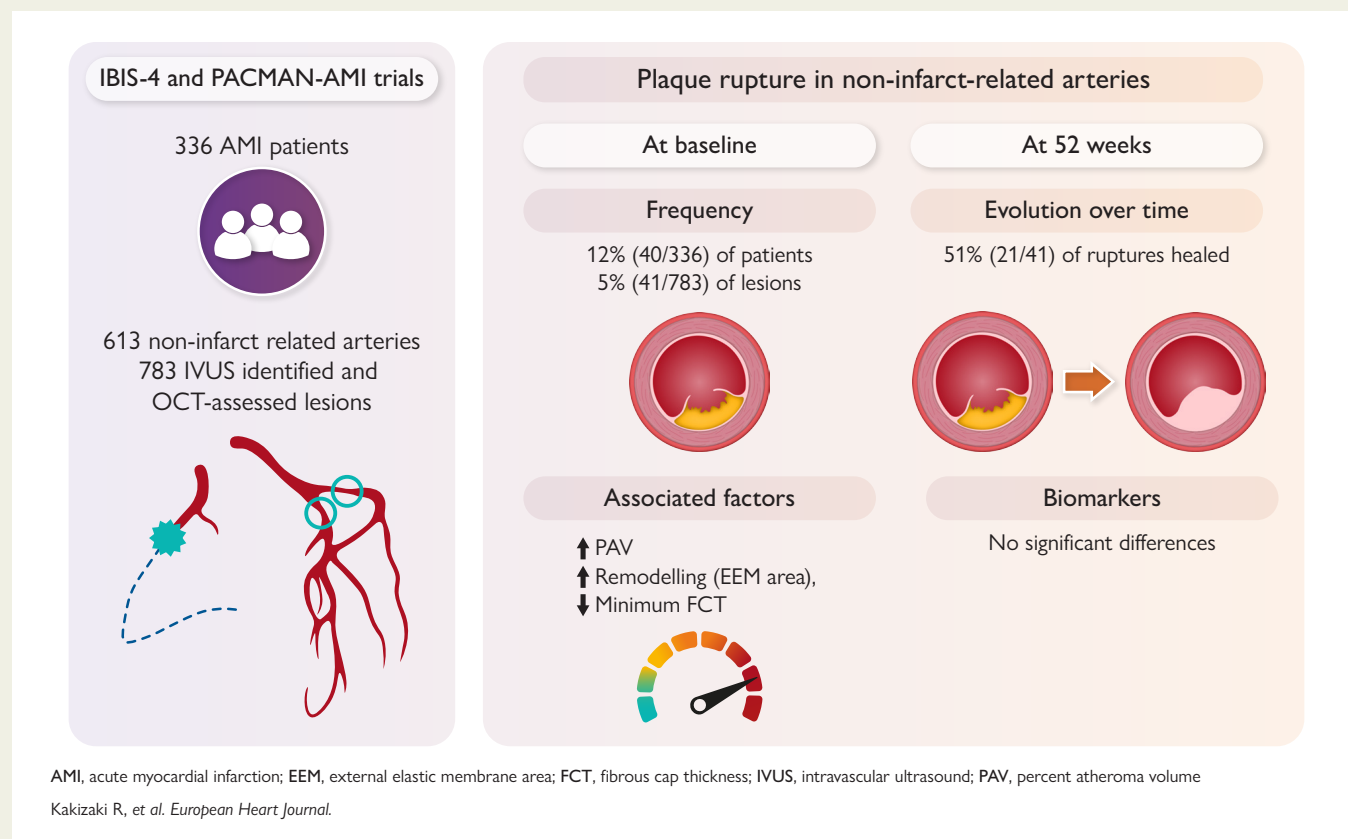
What are the baseline lesion characteristics and evolution of clinically silent plaque ruptures in non-obstructive lesions of non-infarct-related arteries (non-IRAs) among patients with acute myocardial infarction? What baseline morphological features are associated with new-onset silent plaque ruptures?

Key Finding

Ruptures were found in 40 of 336 patients. Larger plaque volume, positive remodelling, and thinner fibrous cap were associated with rupture. Out of 41 rupture sites, 21 healed by 52 weeks. Fibroatheroma was the most frequent underlying morphology of new-onset rupture.

Take Home Message

Silent plaque rupture in non-IRA is observed in a sizeable proportion of AMI patients. About half of plaque fissures heal during follow-up. As fibroatheroma is the prevailing precursor of new-onset silent rupture, such patients may benefit from intensive pharmacological treatment.



Keywords

Vulnerable plaque • Optical coherence tomography • Intravascular ultrasound • Near-infrared spectroscopy • Non-culprit lesion • Thin-cap fibroatheroma

Introduction

Plaque rupture is pathophysiologically defined as the disruption of the fibrous cap overlying the lipid core of advanced atherosclerotic plaques. Previous pathological studies have established plaque rupture as the most common mechanism of instability underlying the onset of acute coronary syndrome (ACS).¹⁻³ However, not all plaque ruptures lead to ACS. In the absence of thrombus formation, or if the thrombus volume is insufficient to obstruct coronary blood flow, plaque rupture may not cause clinically evident myocardial ischaemia—a condition known as silent plaque rupture.⁴ Even if not associated with ACS or angina, lesions with plaque rupture may be at high risk of recurrent coronary events, such as subsequent ruptures or disease progression requiring revascularization.⁵⁻⁸ Therefore, the presence of silent plaque rupture has been proposed as a high-risk morphological plaque feature.^{9,10}

Plaque ruptures have been identified *in vivo* by intracoronary imaging as intimal disruptions with cavity formation.¹¹⁻¹³ Optical coherence tomography (OCT) offers particularly high spatial resolution, making it valuable for detecting plaque rupture *in vivo*.¹⁴ Previous studies using various imaging modalities have demonstrated that plaque rupture can be present even in non-culprit lesions of patients with ACS or stable angina.^{12,15,16} However, the frequency of plaque ruptures in non-obstructive lesions of non-infarct-related arteries (non-IRAs), as well as the morphological changes these lesions undergo over time, remain largely unclear. Furthermore, no studies using serial OCT imaging have investigated either the morphological changes in existing plaque ruptures or the baseline plaque morphology of lesions that subsequently develop silent plaque rupture.

The IBIS-4 (Integrated Biomarker Imaging Study-4) and PACMAN-AMI (Effects of the PCSK9 Antibody Alirocumab on Coronary Atherosclerosis in Patients With Acute Myocardial Infarction) trials included patients with acute myocardial infarction (AMI) who underwent serial OCT and intravascular ultrasound (IVUS) imaging of non-IRAs with non-obstructive lesions at baseline and at 52-week follow-up.^{17,18} Using pooled data from these two clinical trials, the present study aimed to (i) assess the frequency and lesion characteristics of plaque rupture in non-obstructive lesions of non-IRAs among patients with AMI, (ii) evaluate morphological changes at 52 weeks, and (iii) investigate the baseline plaque morphology of lesions that lead to new-onset silent plaque ruptures by 52 weeks.

Methods

Study population

The IBIS-4 trial (NCT00962416) was a prospective, multicentre cohort study designed to investigate the effects of high-dose statin therapy on coronary plaques. The PACMAN-AMI trial (NCT03067844) was an investigator-initiated, multicentre, randomized, double-blind clinical trial evaluating the impact of proprotein convertase subtilisin/kexin Type 9 (PCSK9) inhibitor, in addition to a high-intensity statin therapy, on coronary plaque characteristics. The study designs and primary results of the IBIS-4^{17,19} and PACMAN-AMI trials^{18,20} have been reported previously. IBIS-4 enrolled 103 patients, while PACMAN-AMI enrolled 300 patients who underwent primary percutaneous coronary intervention (PCI) of the culprit lesion for AMI. Both IBIS-4 and PACMAN-AMI enrolled

patients with AMI who underwent successful PCI of the culprit lesion. All patients received high-intensity statin therapy (rosuvastatin therapy 40 mg daily); in PACMAN-AMI, patients were additionally randomized in a double-blind fashion to alirocumab or placebo on top of statin therapy.

Of the 403 patients enrolled in the two clinical trials, 77 patients without baseline OCT images (51 patients) or without an IVUS-defined lesion (16 patients) at baseline were excluded, leaving 336 patients who underwent OCT imaging of non-IRAs with non-obstructive lesions (<50% by visual estimate) at the time of the index event for the present substudy. All participants provided written informed consent, and the study protocols were approved by the ethics committee at each participating institution.

Imaging analysis

All intracoronary imaging analyses in the IBIS-4 and PACMAN-AMI trials were performed in the same independent core laboratories (IVUS, Cardialysis, Rotterdam, the Netherlands; OCT, Bern University Hospital, Bern, Switzerland) by several experienced analysts. Details regarding image acquisition and analysis are provided in the [Supplementary Methods](#). Plaque rupture was defined by OCT as a discontinuity of the intimal layer establishing a communication between a cavity and the coronary lumen.¹⁰⁻¹³ To assess morphological changes at sites of plaque rupture, cross-sectional matching was manually performed using anatomical landmarks (e.g. side branches and calcifications) to identify corresponding frames between baseline and 52-week follow-up OCT images. Healing of plaque rupture was defined as the disappearance of both the flap and cavity structure at the rupture site.

An IVUS-defined lesion was characterized as a segment ≥ 3 mm in length with a plaque burden $\geq 40\%$ and was considered distinct when the separation between adjacent lesions exceeded 5 mm.^{21,22} IVUS and OCT images were co-registered based on anatomical landmarks using dedicated matching software (IvusOctRegistration, Version 16, Medis, Leiden, the Netherlands). Near-infrared spectroscopy (NIRS) imaging was performed in the PACMAN-AMI cohort.

Key intracoronary imaging measurements included percent atheroma volume (PAV), normalized total atheroma volume (TAV), minimum lumen area (MLA), and mean external elastic membrane (EEM) area by IVUS; minimum fibrous cap thickness (FCT), mean FCT, mean macrophage angle, maximum lipid angle, and lipid index by OCT; and the maximum lipid-core burden index within any 4 mm segment ($\text{maxLCBI}_{4\text{mm}}$) by NIRS.

Study endpoints

The key endpoint was prevalence of plaque rupture assessed using OCT in non-IRA lesions at baseline and 52-week follow-up. Additionally, clinical characteristics, biochemical parameters (including inflammatory biomarkers, as detailed in the [Supplementary Methods](#)), and intracoronary imaging findings were compared between lesions with and without plaque rupture. Plaque morphology was evaluated at the matched cross-sectional frame where a rupture was identified either at baseline or at follow-up.

Statistical analysis

Continuous variables are presented as mean (standard deviation) or median [interquartile range], depending on distribution. Categorical variables are expressed as counts (percentages). Between-group comparisons for baseline clinical characteristics and baseline biomarkers were conducted using Student's *t*-tests, Wilcoxon-Mann-Whitney tests, or Fisher's exact tests, as appropriate. A two-sided *P*-value $< .05$ was considered statistically significant.

Analyses of imaging endpoints were conducted at the lesion level using mixed-effect models on values at baseline, at follow-up, and on the change between baseline and Week 52. Patient identity was included as random intercept to account for the multiple lesions per patient. Models conducted on the change were adjusted for the baseline imaging value to control for potential between-group differences at baseline. Values are presented as lesion-level raw mean (SD) or lesion-level raw mean change [95% confidence interval (CI)]. Marginal differences in change between groups are estimated differences extracted from the mixed-effect models at the mean of the baseline covariate.

A multivariable logistic regression analysis was performed to identify baseline imaging parameters associated with baseline plaque rupture, at the lesion level. Covariates were baseline PAV on IVUS, baseline EEM area on IVUS, presence of fibroatheroma on OCT, minimum FCT on OCT, and mean macrophage angle on OCT based on clinical expertise and mechanistic considerations. Statistical tests were two-sided and the significance level was set to .05. All statistical analyses were performed using Stata version 17 (StataCorp LLC, College Station, TX) and R version 4.4.1 (R Core Team).

Results

Frequency of plaque rupture

A total of 783 IVUS-defined lesions from 613 non-IRAs in 336 patients were analysed at baseline. Plaque rupture in non-obstructive lesions of non-IRAs was identified at 46 sites across 41 (5%) of the 783 lesions in 40 (12%) of the 336 patients, with five lesions exhibiting multiple plaque rupture sites. Thrombus was present in 10 (24%) of the 41 lesions with plaque rupture, of which nine were red thrombus and one was white thrombus on OCT. In quantitative coronary angiography, the mean % diameter stenosis of lesions with plaque rupture was $34.5 \pm 11.4\%$, and three lesions had a % diameter stenosis between 50% and 60%. Of the baseline cohort, 742 (95%) of the 783 lesions from 580 non-IRAs in 323 (96%) of the 336 patients underwent serial intracoronary imaging at both baseline and 52-week follow-up (see [Supplementary data online, Figure S1](#)). At 52-week follow-up, 30 rupture sites were identified in 30 (4%) of the 742 lesions and in 28 (9%) of the 323 patients. Of these, 20 rupture sites had already been present at baseline, while 10 were new-onset ruptures.

Patient characteristics

Baseline clinical characteristics of patients with and without plaque rupture are shown in [Table 1](#). There were no significant differences in clinical characteristics between patients with and without plaque rupture. Biochemical parameters, including lipid profiles and inflammatory biomarkers, were comparable between the two groups ([Table 2](#); [Supplementary data online, Table S1](#)).

Clinical characteristics and biochemical findings of patients with and without plaque rupture at 52 weeks are shown in [Supplementary data online, Table S2](#). Patients with rupture at 52 weeks exhibited higher estimated glomerular filtration rate levels at follow-up.

Lesion characteristics

Lesion-level intracoronary imaging findings for lesions with and without plaque rupture at baseline are reported in [Table 3](#). Lesions with plaque rupture at baseline had greater PAV

[$53.3 \pm 6.4\%$ vs $49.5 \pm 5.8\%$; estimated difference (95% CI), 3.6 (1.9–5.4); $P < .001$], smaller minimum FCT [$70 \pm 49 \mu\text{m}$ vs $116 \pm 84 \mu\text{m}$; estimated difference (95% CI), -43 (-75 to -11); $P = .009$], and higher maxLCBI_{4mm} [401 ± 202 vs 226 ± 197 ; estimated difference (95% CI), 178 (93–263); $P < .001$] at baseline compared with those without. There was no significant difference in baseline mean macrophage angle [$58^\circ \pm 34^\circ$ vs $48^\circ \pm 31^\circ$; estimated difference (95% CI), 7 (-2 –16); $P = .109$] between lesions with and without plaque rupture at baseline. While baseline MLA was comparable between groups [$5.5 \pm 2.3 \text{ mm}^2$ vs $5.7 \pm 2.9 \text{ mm}^2$; estimated difference (95% CI), -0.2 (-1.1 –.6); $P = .570$], lesions with plaque rupture at baseline had a significantly larger baseline EEM area [$20.5 \pm 4.8 \text{ mm}^2$ vs $15.7 \pm 5.6 \text{ mm}^2$; estimated difference (95% CI), 4.1 (2.5–5.7); $P < .001$] than those without. Lesions with plaque rupture demonstrated significantly smaller reduction in normalized TAV [$-8.3 \pm 24.5 \text{ mm}^2$ vs $-13.1 \pm 16.4 \text{ mm}^2$; estimated difference (95% CI), 8.5 (3.1–13.9); $P = .002$] and mean EEM area [$1.1 \pm 2.5 \text{ mm}^2$ vs $-0.7 \pm 1.4 \text{ mm}^2$; estimated difference (95% CI), .93 (.48–1.38); $P < .001$], compared with lesions without plaque rupture. Lesions with plaque rupture more frequently had thin-cap fibroatheroma (TCFA) and less frequently had fibrous plaque as the baseline lesion type compared with those without plaque rupture. Among 38 lesions with plaque rupture, 17 (45%) were TCFA, 8 (21%) thick-cap fibroatheroma (ThCFA), 10 (26%) fibrocalcific plaque, and 3 (8%) fibrous plaque, and none were normal, whereas among the 660 lesions without plaque rupture, the corresponding numbers were 60 (9%), 226 (34%), 176 (27%), 186 (29%), and 9 (1%), respectively ($P < .001$; [Figure 1](#)).

Lesion-level imaging characteristics of lesions with vs without plaque rupture at 52 weeks are presented in [Supplementary data online, Table S3](#). At baseline, lesions with plaque rupture at 52 weeks showed greater PAV [$51.8 \pm 6.1\%$ vs $49.6 \pm 5.7\%$; estimated difference (95% CI), 2.3 (.3–4.4), $P = .025$], smaller minimum FCT [$68 \pm 48 \mu\text{m}$ vs $116 \pm 85 \mu\text{m}$; estimated difference (95% CI), -44 (-84 to -4); $P = .031$], larger mean macrophage angle [$62^\circ \pm 46^\circ$ vs $50^\circ \pm 30^\circ$; estimated difference (95% CI), 12 (1–23); $P = .034$], and higher maxLCBI_{4mm} [408 ± 201 vs 227 ± 197 ; estimated difference (95% CI), 189 (95–284); $P < .001$] at baseline. The baseline mean EEM area was larger in lesions with plaque rupture at 52 weeks [$20.0 \pm 4.7 \text{ mm}^2$ vs $15.8 \pm 5.7 \text{ mm}^2$; estimated difference (95% CI), 3.3 (1.3–5.2); $P < .001$], while MLA was comparable [$5.6 \pm 2.5 \text{ mm}^2$ vs $5.7 \pm 2.9 \text{ mm}^2$; estimated difference (95% CI), -0.4 (-1.4 –.6); $P = .731$].

Factors associated with plaque rupture

Multivariable logistic regression analyses are presented in [Table 4](#). In Model 1, which included 698 lesions with baseline IVUS and OCT data, PAV (per 1% increase; OR, 1.11; 95% CI, 1.05–1.18; $P < .001$), mean EEM area (per 1 mm^2 increase; OR, 1.17; 95% CI, 1.10–1.24; $P < .001$), and the presence of fibroatheroma (OR, 2.46; 95% CI, 1.16–5.48; $P = .022$) were independently associated with plaque rupture at baseline.

In Model 2, which included 352 lesions with measurable FCT and macrophage accumulation data, PAV (per 1% increase; OR, 1.14; 95% CI, 1.05–1.26; $P = .003$), mean EEM area (per 1 mm^2 increase; OR, 1.23; 95% CI, 1.13–1.35; $P < .001$), and minimum FCT (per 10 μm increase; OR, .85; 95% CI, .72–.97; $P = .031$) remained

Table 1 Baseline clinical characteristics in patients with vs without plaque rupture at baseline

	Overall N = 336	Plaque rupture(+) N = 40	Plaque rupture(-) N = 296	P-value			
Patients							
Age, years	336	58.1 ± 9.5	40	56.5 ± 8.7	296	58.3 ± 9.6	.27
Female, n (%)	336	48 (14.3)	40	3 (7.5)	296	45 (15.2)	.24
BMI, kg/m ²	336	28.0 ± 4.2	40	28.8 ± 4.6	296	27.9 ± 4.1	.21
Cardiovascular risk factors and medical history, n (%)							
Diabetes mellitus	336	36 (10.7)	40	6 (15.0)	296	30 (10.1)	.41
Hypertension	336	149 (44.3)	40	16 (40.0)	296	133 (44.9)	.61
Hyperlipidaemia	336	240 (71.4)	40	31 (77.5)	296	209 (70.6)	.46
Smoking	336	188 (56.0)	40	23 (57.5)	296	165 (55.7)	.87
Family history of CAD or CVD	333	110 (32.7)	40	13 (32.5)	293	97 (32.8)	>.99
Chronic kidney disease (eGFR < 60 mL/min)	332	12 (3.6)	39	0 (.0)	293	12 (4.1)	.37
Previous myocardial infarction	336	8 (2.4)	40	0 (.0)	296	8 (2.7)	.60
Previous PCI	336	8 (2.4)	40	0 (.0)	296	8 (2.7)	.60
History of stroke	336	4 (1.2)	40	0 (.0)	296	4 (1.4)	>.99
Peripheral artery disease	336	5 (1.5)	40	1 (2.5)	296	4 (1.4)	.47
Type of acute myocardial infarction, n (%)							.86
STEMI	336	223 (66.4)	40	26 (65.0)	296	197 (66.6)	
NSTEMI	336	113 (33.6)	40	14 (35.0)	296	99 (33.4)	
Medication, n (%)							
Antithrombotic therapy							
Aspirin	336	28 (8.3)	40	3 (7.5)	296	25 (8.4)	>.99
P2Y12 inhibitor	336	8 (2.4)	40	1 (2.5)	296	7 (2.4)	>.99
Oral anticoagulation ^a	245	3 (.9)	28	0 (.0)	217	3 (1.0)	>.99
Statin	336	42 (12.5)	40	6 (15.0)	296	36 (12.2)	.61
Other lipid-lowering medication	336	3 (.9)	40	0 (.0)	296	3 (1.0)	>.99
β-blocker	336	28 (8.3)	40	0 (.0)	296	28 (9.5)	.035
ACEI	336	32 (9.5)	40	1 (2.5)	296	31 (10.5)	.15
ARB	336	41 (12.2)	40	5 (12.5)	296	36 (12.2)	>.99
LVEF, %	295	51.5 ± 10.4	257	51.2 ± 8.7	38	51.6 ± 10.6	.83

Values are count (%), mean ± standard deviation. The plaque rupture (+) category includes patients that had ≥1 lesion with plaque rupture while the plaque rupture (-) category includes patients that had no plaque rupture.

ACEI, angiotensin-converting enzyme inhibitor; ARB, angiotensin II receptor blocker; BMI, body mass index; CAD, coronary artery disease; CVD, cardiovascular disease; LVEF, left ventricular ejection fraction; NSTEMI, non-ST-segment elevation myocardial infarction; PCI, percutaneous coronary intervention; STEMI, ST-segment elevation myocardial infarction.

^aThese variables are tested only in PACMAN-AMI cohort (patients with plaque rupture, 28; patients without plaque rupture, 245).

independent predictors of plaque rupture at baseline. In contrast, the mean macrophage angle was not significantly associated (per 10° increase; OR, 1.03; 95% CI, .90–1.18; *P* = .633).

Morphological change of plaque ruptures identified at baseline

Among 41 rupture sites in 38 lesions with serial OCT assessment, 21 ruptures (51%) in 20 lesions had healed at 52 weeks. Plaque

morphologies at the cross-sections with healed plaque ruptures were fibrous plaque in 13 (62%) of the 21 ruptures, layered plaque in 6 (29%) of the 21 ruptures, and ThCFA in 2 (10%) of the 21 ruptures at 52-week follow-up (*Figure 2A*). Of the six lesions with plaque rupture that evolved into a layered plaque at follow-up, thrombus was observed at baseline in two lesions. Representative images of morphological change of rupture sites identified at baseline are shown in *Figure 2B*.

Table 2 Baseline biochemical findings in patients with vs without plaque rupture at baseline

		Overall N = 336		Plaque rupture(+) N = 40		Plaque rupture(-) N = 296		Difference (95% CI)	P-value
eGFR, mL/min/1.73 m ²	332	111.4 ± 36.2	39	121.9 ± 38.8	293	110.0 ± 35.6	11.92 (-.16-23.99)	.05	
Cholesterol, mmol/L									
Total	335	4.3 ± 1.8	40	4.3 ± 1.9	295	4.3 ± 1.8	-.03 (-.63-.58)	.92	
LDL	335	3.2 ± 1.5	40	3.2 ± 1.5	295	3.2 ± 1.5	.05 (-.43-.53)	.85	
HDL	335	.8 ± .5	40	.7 ± .5	295	.8 ± .5	-.10 (-.28-.07)	.23	
Non-HDL-cholesterol, mmol/L	335	3.5 ± 1.5	40	3.5 ± 1.6	295	3.4 ± 1.5	.07 (-.43-.57)	.79	
Triglycerides, mmol/L	335	.9 ± 1.0	40	1.0 ± 1.0	295	.9 ± 1.0	.09 (-.23-.42)	.57	
Lipoprotein(a), nmol/L ^a	245	19.0 [91.0]	28	13.0 [75.0]	217	20.0 [96.0]	-6.00 [-30.97-18.97]	.17	
Apolipoprotein AI, mg/dL ^a	245	1.1 ± .2	28	1.1 ± .2	217	1.1 ± .2	-.05 (-.12-.03)	.20	
Apolipoprotein B, mg/dL ^a	245	1.1 ± .2	28	1.2 ± .2	217	1.1 ± .2	.05 (-.04-.14)	.26	
High-sensitivity C-reactive protein, mg/L	294	1.8 [3.3]	33	1.5 [2.9]	261	1.9 [3.3]	-.44 [-1.40-.52]	.68	
HbA1c, % ^a	234	5.8 ± 1.0	31	6.0 ± 1.1	203	5.8 ± .9	.16 (-.21-.53)	.40	
IL-6 ^a	231	3.6 ± 1.2	27	3.8 ± 1.1	204	3.6 ± 1.2	.23 (-.25-.72)	.35	
MMP-12 ^a	234	6.8 ± .8	27	6.6 ± .7	207	6.8 ± .8	-.23 (-.53-.07)	.14	
TNFα ^a	231	2.8 ± .5	27	2.8 ± .5	204	2.8 ± .4	-.03 (-.21-.15)	.74	
IFNγ ^a	231	6.0 ± 1.0	27	5.9 ± .8	204	6.0 ± 1.0	-.10 (-.50-.31)	.63	

Values are count (%), mean ± standard deviation or median [interquartile range]. Difference (95%) shows the mean difference (95% CI), risk difference (95% CI), or median difference [95% CI]. The plaque rupture (+) category includes patients that had ≥1 lesion with plaque rupture while the plaque rupture (-) category includes patients that had no plaque rupture.

CI, confidence interval; eGFR, estimated glomerular filtration rate; HbA1c, glycated haemoglobin; IFNγ, interferon gamma; IL, interleukin; MMP, matrix metalloproteinase; TNFα, tumour necrosis factor alpha.

^aThese variables are tested only in PACMAN-AMI cohort (patients with plaque rupture, 28; patients without plaque rupture, 245). Unit: NPX (normalized protein expression) by Olink assay.

Baseline morphology of new-onset silent plaque ruptures

Among 30 rupture sites in 30 lesions observed at 52-week follow-up, 10 rupture sites in 10 lesions were newly found. Baseline plaque morphologies of these new-onset silent plaque ruptures were TCFA in five rupture sites (50%), ThCFA in two rupture sites (20%), layered plaque in two rupture sites (20%), and haematoma in one rupture site (10%) (*Figure 3A*). Representative images of baseline morphology of new-onset plaque ruptures are shown in *Figure 3B*. Among the 10 lesions with thrombus, only one lesion showed persistent thrombus at follow-up, and this lesion exhibited a new plaque rupture.

Clinical outcomes

Clinical outcomes at 1 year are shown in [Supplementary data online, Table S4](#). The composite of death, any MI, or ischaemia-driven revascularization occurred in 4 (10%) of the 40 patients with plaque rupture and in 41 (14%) of the 296 patients without plaque rupture in non-IRAs. Ischaemia-driven lesion revascularization was performed in 1 (3%) of the 40 patients with plaque rupture and in 20 (7%) of the 296 patients without plaque rupture.

Discussion

This is the first study to investigate the lesion characteristics and morphological evolution of clinically silent plaque ruptures in non-IRAs of patients with AMI using serial multimodality intracoronary imaging. The main findings of the present study are the following: (i) plaque rupture in non-obstructive lesions of non-IRAs was identified in 40 (12%) of the 336 patients and 41 (5%) of the 783 lesions at baseline; (ii) lesions with plaque rupture at baseline exhibited greater plaque volume, thinner fibrous cap, and greater lipid burden compared with those without; (iii) greater PAV, larger EEM area, and smaller FCT were independently associated with the presence of plaque rupture at baseline; (iv) 21 (51%) of the 41 plaque ruptures transitioned into stabilized morphologies, predominantly fibrous plaques; and (v) new-onset silent plaque rupture at follow-up was observed in 10 lesions, with TCFA as the most frequent underlying plaque type at baseline (see *Structured Graphical Abstract*).

Frequency of lesions with plaque rupture

The frequency of multivessel instability—defined in this study as the presence of plaque rupture in non-IRAs—was lower than

Table 3 Lesion-level intracoronary imaging findings in lesions with vs without plaque rupture at baseline

Time point	Sample size	Plaque rupture(+)	Sample size	Plaque rupture(-)	Difference (95%CI)	P-value
Target vessel, n (%)	41		742			.072
Left anterior descending		18 (44)		248 (33)		
Left circumflex		8 (20)		271 (37)		
Right coronary artery		15 (37)		223 (30)		
Intravascular ultrasound						
Percent atheroma volume, %						
Baseline	41	53.3 ± 6.4	740	49.5 ± 5.8	3.6 (1.9–5.4)	<.001
Follow-up	37	50.5 ± 6.8	707	46.3 ± 7.6	4.1 (1.8–6.5)	<.001
Change	37	–2.7 ± 3.6	705	–3.2 ± 5.2	.7 (–.9–2.4)	.389
Normalized total atheroma volume, mm ³						
Baseline	41	186.9 ± 52.6	740	131.5 ± 49.9	47.9 (33.4–62.5)	<.001
Follow-up	37	180.5 ± 66.1	707	117.4 ± 48.4	53.6 (38.5–68.8)	<.001
Change	37	–8.3 ± 24.5	705	–13.1 ± 16.4	8.5 (3.1–13.9)	.002
Mean atheroma area, mm ²						
Baseline	41	10.9 ± 2.9	740	7.8 ± 2.8	2.8 (2.0–3.7)	<.001
Follow-up	37	10.5 ± 3.8	707	7.0 ± 2.7	3.2 (2.3–4.1)	<.001
Change	37	–.5 ± 1.5	705	–.8 ± 1.0	.6 (–.2–.9)	<.001
Mean EEM area, mm ²						
Baseline	41	20.5 ± 4.8	740	15.7 ± 5.6	4.1 (2.5–5.7)	<.001
Follow-up	37	20.8 ± 6.1	707	15.1 ± 5.4	4.8 (3.1–6.5)	<.001
Change	37	.1 ± 2.5	705	–.7 ± 1.4	.9 (–.5–1.4)	<.001
Min lumen area, mm ²						
Baseline	41	5.5 ± 2.3	740	5.7 ± 2.9	–.2 (–1.1–.6)	.570
Follow-up	37	6.0 ± 2.5	707	5.7 ± 3.0	.1 (–.8–1.1)	.776
Change	37	.3 ± .9	705	–.0 ± 1.1	.3 (–.0–.7)	.062
Optical coherence tomography						
Minimum FCT, μm						
Baseline	27	70 ± 49	369	116 ± 84	–43 (–75 to –11)	.009
Follow-up	24	109 ± 74	349	160 ± 93	–55 (–93 to –18)	.004
Change	24	50 ± 66	323	46 ± 96	–27 (–63–8)	.133
Mean FCT, μm						
Baseline	27	272 ± 108	369	325 ± 109	–48 (–91 to –5)	.027
Follow-up	24	356 ± 96	349	391 ± 109	–37 (–82–7)	.096
Change	24	105 ± 103	323	68 ± 126	–16 (–59–27)	.473
Mean macrophage angle, °						
Baseline	38	58 ± 34	555	48 ± 31	7 (–2–16)	.109
Follow-up	36	41 ± 27	471	32 ± 26	8 (0–16)	.048
Change	36	–19 ± 23	450	–17 ± 28	4 (–3–11)	.280
Maximum lipid angle, ° ^a						

Continued

Table 3 Continued

Time point	Sample size	Plaque rupture(+)	Sample size	Plaque rupture(-)	Difference (95%CI)	P-value
Baseline	22	210 ± 96	320	146 ± 63	65 (36–93)	<.001
Follow-up	21	192 ± 91	305	119 ± 60	77 (49–104)	<.001
Change	21	–25 ± 83	294	–28 ± 55	35 (13–58)	.002
Lipid index^a						
Baseline	22	1167 ± 820	320	558 ± 609	645 (378–913)	<.001
Follow-up	21	960 ± 772	305	427 ± 468	563 (347–781)	<.001
Change	21	–256 ± 404	294	–150 ± 314	95 (–19–210)	.101
Near-infrared spectroscopy						
maxLCBI_{4mm}^a						
Baseline	20	401 ± 202	559	226 ± 197	178 (93–263)	<.001
Follow-up	19	272 ± 238	560	174 ± 184	109 (28–190)	.009
Change	19	–130 ± 216	555	–51 ± 161	–1 (–67–65)	.984

Values are lesion-level raw mean ± standard deviation or lesion-level raw mean change ± standard deviation. Sample size refers to the number of lesions. Between-group differences (95% CI) are extracted from mixed-effect models. Normalized total atheroma volume was calculated as mean atheroma area multiplied by the median length of the regions of interest.

CI, confidence interval; EEM, external elastic membrane; FCT, fibrous cap thickness; maxLCBI_{4mm}, maximum lipid core burden index within 4 mm.

^aThese variables were tested only in the PACMAN-AMI cohort.

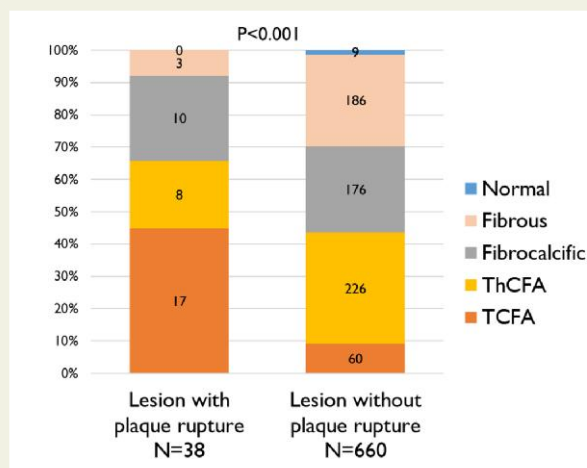


Figure 1 Optical coherence tomography-defined lesion types at the index event in lesions with vs without plaque rupture. Thin-cap fibroatheroma was observed in 45% ($n = 17$) of lesions with rupture vs 9% ($n = 60$) without, thick-cap fibroatheroma in 21% ($n = 8$) vs 34% ($n = 226$), fibrocalcific plaque in 26% ($n = 10$) vs 27% ($n = 176$), fibrous plaque in 8% ($n = 3$) vs 29% ($n = 186$), and normal morphology in 0% ($n = 0$) vs 1% ($n = 9$), respectively

reported in previous studies. Non-culprit plaque rupture was identified in 24% of AMI patients in the study by Vergallo et al.,¹³ 17.6% of ACS patients in the study by Sugiyama et al.,²³ and 14.3% of ST-segment elevation myocardial

infarction (STEMI) patients in the study by Cao et al.²⁴ The lower frequency observed in our cohort may reflect differences in lesion severity. The IBIS-4 and PACMAN-AMI trials included only lesions with <50% diameter stenosis on angiography,^{17,18} whereas the aforementioned studies have included culprit vessels and more advanced lesions. Prior reports have suggested a correlation between lesion severity and the frequency of plaque rupture.^{7,23,25} Given the milder stenosis and the absence of culprit-vessel and distal-segment assessment in our study, the lower frequency of non-culprit plaque rupture is plausible.

Patient and lesion characteristics of those with plaque rupture

Previous studies have demonstrated that patients with non-culprit plaque rupture tend to have a higher prevalence of ACS, male sex, prior PCI, and elevated body mass index, compared with those without rupture.^{7,26} In contrast, our study did not identify significant differences in clinical characteristics between patients with and without non-culprit plaque rupture. Elevated LDL cholesterol (LDL-C) has also been reported as a factor associated with non-culprit plaque rupture.¹³ Moreover, inflammatory biomarkers may be linked to non-culprit plaque rupture.²⁷ However, in the present study, no significant differences were observed in biochemical parameters, including lipid profiles (e.g. LDL-C, lipoprotein(a), and apolipoprotein B) and inflammatory markers (e.g. high-sensitivity C-reactive protein, interleukin-6, and tumour necrosis factor alpha). Consequently, predicting multivessel instability based solely on circulating biomarkers may be challenging in AMI patients. Nevertheless, the potential association between

Table 4 Multivariable analysis to identify predictors of lesion with plaque rupture at baseline

Model including all lesions				Model including only lesions with measured FCT			
Predictors of plaque rupture	Sample size	Odds ratio (95% CI)	P-value	Predictors of plaque rupture	Sample size	Odds ratio (95% CI)	P-value
Baseline PAV (per 1%)	698	1.11 (1.05–1.18)	<.001	Baseline PAV (per 1%)	352	1.14 (1.05–1.26)	.003
Baseline mean EEM area (per 1 mm ²)	698	1.17 (1.10–1.24)	<.001	Baseline mean EEM area (per 1 mm ²)	352	1.23 (1.13–1.35)	<.001
Baseline fibroatheroma	698	2.46 (1.16–5.48)	.022	Baseline minimum FCT (per 10 μm)	352	.85 (.72–.97)	.031
				Baseline mean macrophage angle (per 10°)	352	1.03 (.90–1.18)	.633

Values are odds ratio (95% CI) and associated P-values extracted from a multivariable logistic model. CI, confidence interval; EEM, external elastic membrane; FCT, fibrous cap thickness; PAV, percent atheroma volume.

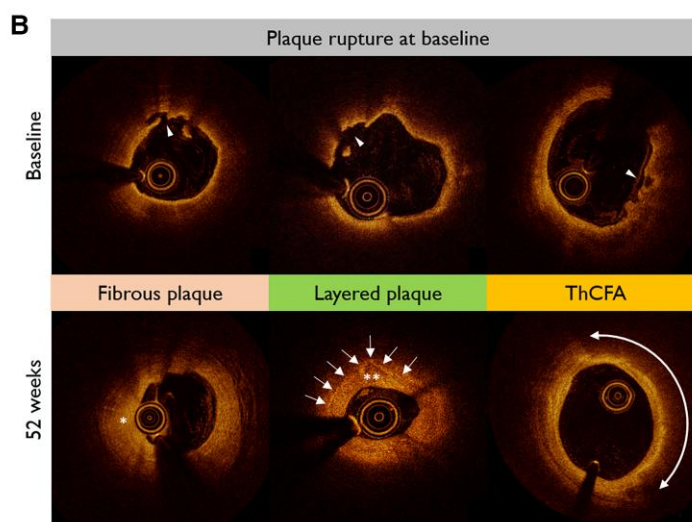
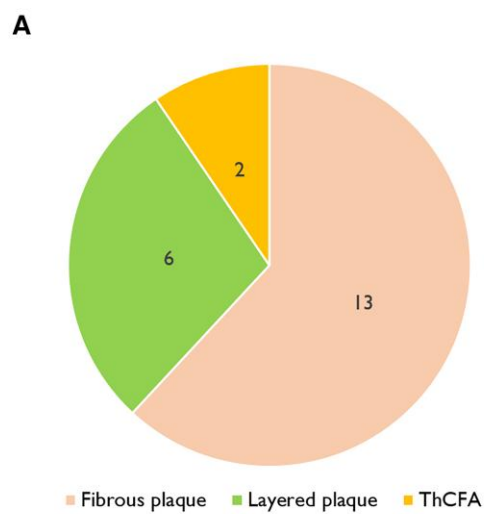


Figure 2 Evolution of ruptured fibroatheroma into healed ruptures at 52-week follow-up. (A) The plaque morphology at 52-week follow-up of lesions that showed plaque rupture at baseline is shown in this pie graph. (B) Representative images of ruptured thin-cap fibroatheroma at baseline that evolved into healed plaque with different morphology at 52-week follow-up. Arrowheads highlight rupture sites, defined as intimal disruption with cavity formation. Single asterisk indicates sites where ruptures evolved into fibrous tissue, and double asterisks indicate transformation into the layered plaque. Arrows highlight the layered structure of the plaque, and the double-headed arrow indicates the extent of a thick-cap fibroatheroma. ThCFA, thick-cap fibroatheroma

circulating biomarkers and non-culprit plaque ruptures warrants further investigation in broader patient populations, including those with stable or unstable angina and severer non-culprit lesions and based on collection of local (vs systemic) markers.

Our findings regarding lesion characteristics are consistent with previous studies, which have shown that lesions with plaque rupture tend to have higher plaque burden, thinner fibrous cap, greater lipid content, and longer lesion length compared with lesions without rupture.^{7,12,13,23} The present study using multimodality intracoronary imaging demonstrated that specific lesion characteristics were associated with the presence of

plaque rupture at the lesion level; in particular, greater PAV, larger EEM area, and smaller FCT were independently associated with rupture at baseline within the same cohort. In contrast, MLA did not differ between lesions with and without plaque rupture. This may reflect the inclusion of only non-obstructive lesions in non-IRAs, which likely excluded lesions with critically small MLA. Alternatively, it may indicate that these ruptures did not lead to significant luminal obstruction, as MLA was adequately preserved. These findings suggest that plaque rupture is more likely to occur in lesions with advanced atherosclerosis and positive remodelling, where high-risk features may promote rupture independently of luminal narrowing.

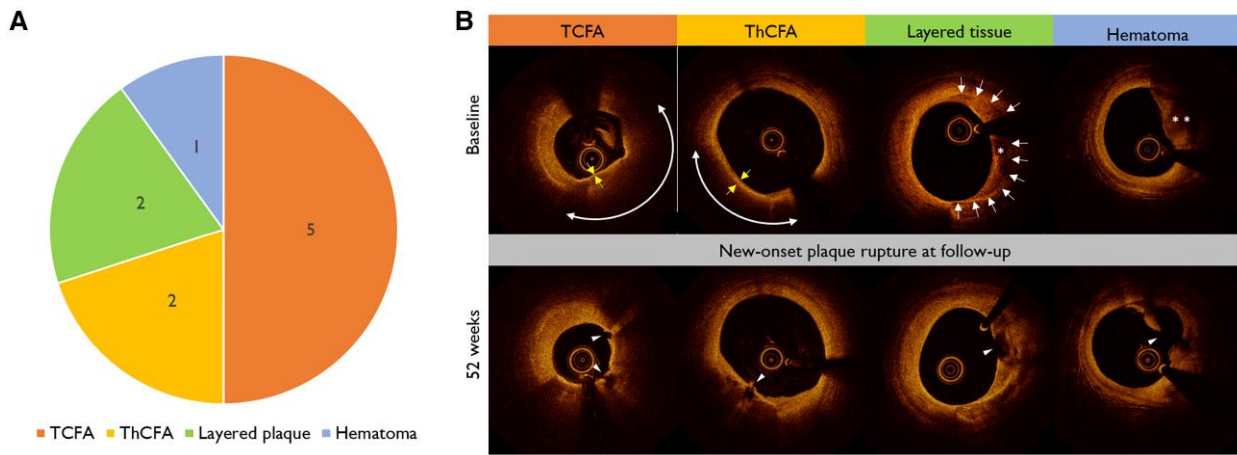


Figure 3 Baseline morphology of new-onset silent plaque ruptures. (A) The baseline plaque morphology of new-onset (at 52 weeks) silent plaque rupture is shown in this pie graph. (B) Representative images of baseline plaque morphologies underlying new-onset silent plaque rupture. Arrowheads highlight rupture sites, defined as intimal disruption with cavity formation. Yellow arrows indicate the fibrous cap thickness of thin-cap fibroatheroma, and double-headed arrows delineate the extent of thick-cap fibroatheroma. White arrows highlight the layered structure of layered plaques. Single asterisk marks layered plaque that became rupture sites, and double asterisks indicate haematoma that served as the rupture site. Abbreviations: TCFA, thin-cap fibroatheroma; ThCFA, thick-cap fibroatheroma

In our study, the reduction in normalized TAV and mean EEM area was significantly smaller in lesions with plaque rupture, despite their larger baseline values. Compared with lesions without rupture, those with plaque rupture may be more prone to limited plaque regression and reverse vessel remodelling in response to lipid-lowering therapy. It is also worth noting that some ruptured lesions were classified as fibrocalcific or fibrous plaques. As lipid pools were not required for the definition of plaque rupture in this study, some older, non-thrombogenic lesions—representing chronic plaque rupture—may have been included.

Morphological change of plaque ruptures

More than half of plaque ruptures identified at baseline healed by 52 weeks, with the majority transitioning to a stabilized plaque morphology, predominantly fibrous plaque. While previous case reports have described healing of plaque ruptures detected by OCT,^{28,29} this is the first study to assess morphological changes using serial OCT imaging. A previous IVUS study reported that 29% of 28 patients with plaque rupture showed evidence of healing after 1 year, with all patients receiving statin therapy.³⁰ The higher frequency of healed ruptures observed in our study may be attributable to the superior spatial resolution of OCT, which enables the detection of smaller ruptures, and the intensive lipid-lowering therapy provided in the IBIS-4 and PACMAN-AMI trial, with all patients receiving high-dose statins—and nearly half received additional therapy with a PCSK9 inhibitor.

Sites of plaque rupture may heal through the organization of thrombus rich in platelets and fibrin, infiltration of smooth muscle cells, and formation of granulation tissue with accumulated proteoglycans and Type III collagen, eventually evolving into layered plaque as observed by OCT.^{31,32} However, in the

present study, less than one-quarter of plaque ruptures transitioned to layered plaques. Several factors may explain this finding, including the relatively low incidence of thrombus [10 (24%) of 41 lesions], the inclusion of older ruptures with unknown timing, and the small size of many rupture cavities. In such rupture sites, the healed area may be small or thin and thus not detectable as layered plaque on OCT. Furthermore, high-dose statin therapy in all patients may have contributed to reductions in lipid content and vascular inflammation, resulting in fibrous plaque morphology in the majority of healed ruptures.

Baseline morphology of new-onset silent plaque ruptures

At the 52-week follow-up, new-onset silent plaque ruptures were observed in 10 lesions, providing a unique opportunity to study in detail the precursor morphology, confirming TCFA as the most frequent underlying plaque type at baseline, consistent with the pathophysiology of plaque rupture.³³ Previous studies have demonstrated a higher incidence of adverse events arising from lesions with TCFA compared with those without,^{8,34} suggesting that plaque rupture may underlie clinical events associated with TCFA.

In addition to fibroatheroma, we also observed layered plaque and haematoma as baseline plaque morphologies in new-onset ruptures. The exact mechanism of plaque rupture in these morphologies remains unclear, but it is likely distinct from that in fibroatheroma. Immature tissue in organized thrombi and haematomas may collapse and cause intimal disruptions with cavities. Plaque ruptures in these morphologies may exhibit different thrombogenicity from those in fibroatheroma, due to the absence of highly thrombogenic lipid cores.

Clinical outcome

The role of non-culprit plaque rupture as an independent high-risk plaque feature remains underevaluated. In our study, we found a numerically lower rate of ischaemia-driven revascularization in lesions with plaque rupture [1 (3%) of 40 patients] compared with those without [20 (7%) of 296 patients] and no difference in the composite of death, any MI, or ischaemia-driven revascularization between the two groups [4 (10%) of 40 patients vs 41 (14%) of 296 patients]. Similarly, Xing *et al.* reported no significant difference in the baseline prevalence of non-culprit plaque rupture between patients with and without major adverse cardiac events (MACEs).³⁵ More recently, in the individual patient data analysis of the COMBINE and PECTUS studies, the presence of plaque rupture was included in the definition of a 'high-risk plaque' (i.e. presence of at least two pre-specified criteria including lipid arc $\geq 90^\circ$, minimum FCT < 65 μm , and presence of either plaque rupture or thrombus). A higher prevalence of baseline high-risk plaque was found in patients who experienced MACE compared with those who did not, but only 8% of plaques were categorized as high risk due to plaque rupture.⁸ Based on all the above data, clinically silent plaque ruptures do not appear to be associated with excessive risk of future events, and pre-emptive stenting may not be necessary.

Limitations

This study has several limitations. First, lipid pool presence was not required for the definition of plaque rupture, which may have led to the inclusion of older, non-thrombogenic ruptures. As a result, some lesions with plaque ruptures were classified as fibrocalcific or fibrous plaques, and new-onset plaque ruptures were observed in previously healed plaques or haematomas. These findings indicate intimal disruptions in OCT but may not reflect actual plaque rupture as a pathological condition. Second, both patient- and lesion-level selection limit the generalisability of our findings. At the patient level, inclusion was restricted to AMI patients with multivessel disease, which likely enriches the cohort for individuals at increased risk of non-culprit rupture compared with a general, unselected population. At the lesion level, we analysed non-obstructive lesions with <50% diameter stenosis, thereby focusing on plaques at an earlier disease stage and potentially attenuating the observed frequency of plaque rupture at the lesion level. Third, the present study did not include systematic imaging of the entire epicardial coronary artery tree, but focused on the proximal coronary segments, where most vulnerable lesions have been reported to reside.^{36,37} Consequently, plaque ruptures in culprit vessels, in distal vessel segments, or in significant lesions with $\geq 50\%$ stenosis were not evaluated. In contrast, both the IBIS-4 and PACMAN-AMI trials enrolled patients with non-obstructive lesions located in the proximal segments of two non-IRAs, allowing a comprehensive evaluation of plaque rupture at non-obstructive sites in non-IRAs at the patient level. Fourth, differences in treatment regimens, such as the use of PCSK9 inhibitors, may have affected the morphological changes of plaque ruptures. Fifth, the prevalence of plaque rupture in non-culprit lesions may differ depending on whether the culprit lesion was caused by plaque rupture, erosion, or calcified nodule.²³ However, the underlying mechanism of AMI in the culprit lesion

was not assessed in the IBIS-4 and PACMAN-AMI trials. Future studies are needed to investigate this relevant aspect. Sixth, as limitation of intracoronary imaging studies, it cannot be excluded with certainty that passage of guidewires or imaging catheters may have induced iatrogenic plaque injury,^{6,38} although no clinically apparent events consistent with iatrogenic plaque rupture were documented in the IBIS-4 and PACMAN-AMI trials.^{18,39} Further, lesions with intimal disruption without cavity were not defined as plaque rupture in the present study. Finally, 16 lesions with thrombus directly attached to plaques in non-IRAs, without associated plaque rupture, were identified. These were all very small in size (<300 μm), and their clinical significance remains uncertain. Because thrombus in the absence of rupture may represent erosion—and thus multivessel instability—we documented these findings but did not include them in the primary analyses. Importantly, a procedural artefact cannot be excluded: catheter manipulation and prolonged interrogation with multiple intracoronary imaging devices may generate procedure-related thrombus rather than true plaque-associated thrombus.

Conclusions

Optical coherence tomography-detected plaque rupture in non-obstructive lesions of non-IRAs at was present in 12% of AMI patients at the index event. Similar biochemical findings between in patients with and without non-culprit plaque rupture may suggest limited value evaluations in identifying multivessel instability based on systemic markers alone. In contrast, lesion-specific characteristics—including greater plaque burden, positive remodelling, and thinner fibrous cap—were associated with plaque rupture. More than half of these ruptures transitioned into stabilized morphologies, predominantly fibrous plaques. Thin-cap fibroatheroma was the most frequent underlying plaque type in new-onset silent plaque ruptures.

Acknowledgements

The authors thank the staff personnel of the cardiovascular department at participating sites for their invaluable support.

Supplementary data

Supplementary data are available at [European Heart Journal](#) online.

Declarations

Disclosure of Interest

L.R. reported receiving grants from Sanofi, Regeneron, Infraredx, Abbott, Heartflow, Boston Scientific, and Biotronik to Inselspital and speaker fees from Sanofi, Abbott, Amgen, AstraZeneca, Occlutech, Canon, Novo Nordisk, and Medtronic outside the submitted work. R.K. reported receiving consulting fee from Infraredx USA outside the submitted work. F.G.B. reported receiving consulting fee from Abbott and speaker fee from Abbott, Ultragenyx, and Sanofi outside the submitted work. S.L. is employed by the DCR Bern, University of Bern, which has a staff policy of not accepting honoraria or

consultancy fees. However, CTU Bern is involved in the design, conduct, or analysis of clinical studies funded by not-for-profit and for-profit organizations. In particular, pharmaceutical and medical device companies provide direct funding to some of these studies (for an up-to-date list of DCR Bern's conflicts of interest, see https://dcr.unibe.ch/services/terms_conditions/index_eng.html). Y.U. reported receiving grants from Astellas Pharma and personal fees from Abbott Vascular, Amgen, Bayer, Daiichi Sankyo, Kowa, NIPRO, and Novartis, outside the submitted work. S.B. reported research grants to the institution from Abbott and Medis Medical Imaging Systems, speaker fees from Cleerly Inc., and travel fees from Sanofi, outside the submitted work. J.L. reported receiving grants from Boston Scientific, consulting fees from Boston Scientific, speaker fee from Abbott and Boston Scientific, and support for attending meetings and travel from Abbott and owns stock in Novo Nordisk. E.S. declares institutional contracts/grants for which he receives no direct compensation from Abbott; Biosensors Europe SA, Boston Scientific; Edwards Lifesciences; Medtronic; Mixin Medtech (Suzhou) Co., Ltd; Shanghai Microport Medical Co., Ltd; Novo Nordisk A/S; NVT GmbH; Philips Healthcare; Pie Medical Imaging; Shanghai Shenqi Medical Technologies Co., Ltd; and Siemens Healthcare GmbH. E.S. declares being a board member of Cardialysis, European Cardiovascular Research Institute, EU-MDR Cardiovascular Collaboratory, and Academic Research Consortium. A.S.O. received support for travel and attending meetings from MSD and OrphaCare. R.-J.v.G. reported receiving grants from Amgen, Infraredx, AstraZeneca, and Sanofi and personal fees from Infraredx outside the submitted work. C.M.M. reported research grant from Sanofi, Regeneron, and Swiss National Science Foundation for biomarker measuring in the present manuscript and research grants to the institution from Eli Lilly, AstraZeneca, Roche, Amgen, Novartis, Novo Nordisk, and MSD, including speaker or consultant fees—all outside the submitted work. J.F.I. reported receiving institutional grants from Biotronik, SMT, Terumo Corporation, and Concept Medical; consulting fees from Biotronik, ReCor Medical, Cordis, and Medtronic, speaker fees from Biotronik, Biosensors, Concept Medical, Cordis, Medtronic, Penumbra Inc., and ReCor Medical; and support for travel from Biotronik and Medtronic outside the submitted work. D.S. reports personal fees from Sanofi-Aventis (Switzerland) at the time of study conduct and Cook Medical, outside the submitted work. J.D. received institutional grant/research support from Abbott Vascular, Boston Scientific, ACIST Medical, Medtronic, Pie Medical, and ReCor medical and consultancy and speaker fees from Abbott Vascular, Abiomed, ACIST Medical, Boston Scientific, Cardialysis BV, CardiacBooster, Kaminari Medical, ReCor Medical, PulseCath, Pie Medical, Sanofi, Siemens Health Care, and Medtronic. J.D. declares being a Data Safety Monitoring Board member of Co-STAR trial. F.M. is supported by Deutsche Gesellschaft für Kardiologie (DGK), Deutsche Forschungsgemeinschaft (SFB TRR219, Project-ID 322900939), and Deutsche Herzstiftung. He has received scientific support from Ablative Solutions, Medtronic, and ReCor Medical and speaker honoraria/consulting fees from Ablative Solutions, Amgen, AstraZeneca, Bayer, Boehringer Ingelheim, Inari, Medtronic, Merck, ReCor Medical, Servier, and Terumo. T.E. reported receiving speaker fees from Abbott Vascular,

Boston Scientific, and Novo Nordisk outside the submitted work. T.E. declares being an advisory board member of Abbott Vascular and Boston Scientific. I.M.L. has relationships with drug companies including AOP Health, Actelion-Janssen, MSD, United Therapeutics, Pulnovo, Medtronic, INARI, Neutrolis, Novo Nordisk, and Sanofi. In addition to being an investigator in trials involving these companies, relationships include consultancy service, research grants, and membership of scientific advisory boards. K.C.K. reported receiving grants from Sanofi, Regeneron, and Infraredx during the conduct of the study and personal fees from Amgen and Daiichi Sankyo outside the submitted work.

Data Availability

The data set will be available from the corresponding author on reasonable request.

Funding

Nothing to declare.

Ethical Approval

The study protocol was approved by the responsible ethics committees. The trial was conducted in accordance with Good Clinical Practice guidelines and is reported following the Consolidated Standards of Reporting Trials (CONSORT) 2010 reporting guideline statement for parallel-group randomized trial statement.

Pre-registered Clinical Trial Number

The IBIS-4 trial and the PACMAN-AMI trial were registered at www.clinicaltrials.gov (identifier: NCT00962416 and NCT03067844, respectively).

References

- Falk E, Nakano M, Bentzon JF, Finn AV, Virmani R. Update on acute coronary syndromes: the pathologists' view. *Eur Heart J* 2013;**34**:719–28. <https://doi.org/10.1093/eurheartj/ehs411>
- Jia H, Abtahian F, Aguirre AD, Lee S, Chia S, Lowe H, et al. In vivo diagnosis of plaque erosion and calcified nodule in patients with acute coronary syndrome by intravascular optical coherence tomography. *J Am Coll Cardiol* 2013;**62**:1748–58. <https://doi.org/10.1016/j.jacc.2013.05.071>
- Higuma T, Soeda T, Abe N, Yamada M, Yokoyama H, Shibutani S, et al. A combined optical coherence tomography and intravascular ultrasound study on plaque rupture, plaque erosion, and calcified nodule in patients with ST-segment elevation myocardial infarction: incidence, morphologic characteristics, and outcomes after percutaneous coronary intervention. *JACC Cardiovasc Interv* 2015;**8**:1166–76. <https://doi.org/10.1016/j.jcin.2015.02.026>
- Kawai K, Finn AV, Virmani R; Subclinical Atherosclerosis Collaborative. Subclinical atherosclerosis: part 1: what is it? Can it be defined at the histological level? *Arterioscler Thromb Vasc Biol* 2024;**44**:12–23. <https://doi.org/10.1161/ATVBAHA.123.319932>
- Prati F, Romagnoli E, Gatto L, La Manna A, Burzotta F, Ozaki Y, et al. Relationship between coronary plaque morphology of the left anterior descending artery and 12 months clinical outcome: the CLIMA study. *Eur Heart J* 2020;**41**:383–91. <https://doi.org/10.1093/eurheartj/ehz520>
- Erlinge D, Maehara A, Ben-Yehuda O, Bøtker HE, Maeng M, Kjoller-Hansen L, et al. Identification of vulnerable plaques and patients by intracoronary near-infrared spectroscopy and ultrasound (PROSPECT II): a prospective natural history study. *Lancet* 2021;**397**:985–95. [https://doi.org/10.1016/S0140-6736\(21\)00249-X](https://doi.org/10.1016/S0140-6736(21)00249-X)
- Xie Y, Mintz GS, Yang J, Doi H, Iñiguez A, Dangas GD, et al. Clinical outcome of nonculprit plaque ruptures in patients with acute coronary syndrome in the PROSPECT study. *JACC Cardiovasc Imaging* 2014;**7**:397–405. <https://doi.org/10.1016/j.jcmg.2013.10.010>

8. Volleberg R, Rroku A, Mol JQ, Hermanides RS, van Leeuwen M, Berta B, et al. FFR-negative nonculprit high-risk plaques and clinical outcomes in high-risk populations: an individual patient-data pooled analysis from COMBINE (OCT-FFR) and PECTUS-obs. *Circ Cardiovasc Interv* 2025;18:e014667. <https://doi.org/10.1161/CIRCINTERVENTIONS.124.014667>
9. Burzotta F, Leone AM, Aurigemma C, Zambrano A, Zimbardo G, Ariotti M, et al. Fractional flow reserve or optical coherence tomography to guide management of angiographically intermediate coronary stenosis: a single-center trial. *JACC Cardiovasc Interv* 2020;13:49–58. <https://doi.org/10.1016/j.jcin.2019.09.034>
10. Mol JQ, Volleberg R, Belkacemi A, Hermanides RS, Meuwissen M, Protopopov AV, et al. Fractional flow reserve-negative high-risk plaques and clinical outcomes after myocardial infarction. *JAMA Cardiol* 2023;8:1013–21. <https://doi.org/10.1001/jamacardio.2023.2910>
11. Vergallo R, Ren X, Yonetsu T, Kato K, Uemura S, Yu B, et al. Pancoronary plaque vulnerability in patients with acute coronary syndrome and ruptured culprit plaque: a 3-vessel optical coherence tomography study. *Am Heart J* 2014;167:59–67. <https://doi.org/10.1016/j.ahj.2013.10.011>
12. Tian J, Ren X, Vergallo R, Xing L, Yu H, Jia H, et al. Distinct morphological features of ruptured culprit plaque for acute coronary events compared to those with silent rupture and thin-cap fibroatheroma: a combined optical coherence tomography and intravascular ultrasound study. *J Am Coll Cardiol* 2014;63:2209–16. <https://doi.org/10.1016/j.jacc.2014.01.061>
13. Vergallo R, Uemura S, Soeda T, Minami Y, Cho JM, Ong DS, et al. Prevalence and predictors of multiple coronary plaque ruptures: in vivo 3-vessel optical coherence tomography imaging study. *Arterioscler Thromb Vasc Biol* 2016;36:2229–38. <https://doi.org/10.1161/ATVBAHA.116.307891>
14. Araki M, Park SJ, Dauerman HL, Uemura S, Kim JS, Di Mario C, et al. Optical coherence tomography in coronary atherosclerosis assessment and intervention. *Nat Rev Cardiol* 2022;19:684–703. <https://doi.org/10.1038/s41569-022-00687-9>
15. Maehara A, Mintz GS, Bui AB, Walter OR, Castagna MT, Canos D, et al. Morphologic and angiographic features of coronary plaque rupture detected by intravascular ultrasound. *J Am Coll Cardiol* 2002;40:904–10. [https://doi.org/10.1016/S0735-1097\(02\)02047-8](https://doi.org/10.1016/S0735-1097(02)02047-8)
16. Asakura M, Ueda Y, Yamaguchi O, Adachi T, Hirayama A, Hori M, et al. Extensive development of vulnerable plaques as a pan-coronary process in patients with myocardial infarction: an angioscopic study. *J Am Coll Cardiol* 2001;37:1284–8. [https://doi.org/10.1016/S0735-1097\(01\)01135-4](https://doi.org/10.1016/S0735-1097(01)01135-4)
17. Räber L, Koskinas KC, Yamaji K, Taniwaki M, Roffi M, Holmvang L, et al. Changes in coronary plaque composition in patients with acute myocardial infarction treated with high-intensity statin therapy (IBIS-4): a serial optical coherence tomography study. *JACC Cardiovasc Imaging* 2019;12:1518–28. <https://doi.org/10.1016/j.jcmg.2018.08.024>
18. Räber L, Ueki Y, Otsuka T, Losdat S, Häner JD, Lonborg J, et al. Effect of alirocumab added to high-intensity statin therapy on coronary atherosclerosis in patients with acute myocardial infarction: the PACMAN-AMI randomized clinical trial. *JAMA* 2022;327:1771–81. <https://doi.org/10.1001/jama.2022.5218>
19. Räber L, Taniwaki M, Zaugg S, Kelbaek H, Roffi M, Holmvang L, et al. Effect of high-intensity statin therapy on atherosclerosis in non-infarct-related coronary arteries (IBIS-4): a serial intravascular ultrasonography study. *Eur Heart J* 2015;36:490–500. <https://doi.org/10.1093/eurheartj/ehu373>
20. Zanchin C, Koskinas KC, Ueki Y, Losdat S, Häner JD, Bar S, et al. Effects of the PCSK9 antibody alirocumab on coronary atherosclerosis in patients with acute myocardial infarction: a serial, multivessel, intravascular ultrasound, near-infrared spectroscopy and optical coherence tomography imaging study-Rationale and design of the PACMAN-AMI trial. *Am Heart J* 2021;238:33–44. <https://doi.org/10.1016/j.ahj.2021.04.006>
21. Ueki Y, Yamaji K, Losdat S, Karagiannis A, Taniwaki M, Roffi M, et al. Discordance in the diagnostic assessment of vulnerable plaques between radiofrequency intravascular ultrasound versus optical coherence tomography among patients with acute myocardial infarction: insights from the IBIS-4 study. *Int J Cardiovasc Imaging* 2021;37:2839–47. <https://doi.org/10.1007/s10554-021-02272-6>
22. Biccirè FG, Kakizaki R, Koskinas KC, Ueki Y, Häner J, Shibutani H, et al. Lesion-level effects of LDL-C-lowering therapy in patients with acute myocardial infarction: a post hoc analysis of the PACMAN-AMI trial. *JAMA Cardiol* 2024;9:1082–92. <https://doi.org/10.1001/jamacardio.2024.3200>
23. Sugiyama T, Yamamoto E, Bryniarski K, Xing L, Lee H, Isobe M, et al. Nonculprit plaque characteristics in patients with acute coronary syndrome caused by plaque erosion vs plaque rupture: a 3-vessel optical coherence tomography study. *JAMA Cardiol* 2018;3:207–14. <https://doi.org/10.1001/jamacardio.2017.5234>
24. Cao M, Zhao L, Ren X, Wu T, Yang G, Du Z, et al. Pancoronary plaque characteristics in STEMI caused by culprit plaque erosion versus rupture: 3-vessel OCT study. *JACC Cardiovasc Imaging* 2021;14:1235–45. <https://doi.org/10.1016/j.jcmg.2020.07.047>
25. Mori H, Torii S, Kutyna M, Sakamoto A, Finn AV, Virmani R. Coronary artery calcification and its progression: what does it really mean? *JACC Cardiovasc Imaging* 2018;11:127–42. <https://doi.org/10.1016/j.jcmg.2017.10.012>
26. Hong MK, Mintz GS, Lee CW, Kim YH, Lee SW, Song JM, et al. Comparison of coronary plaque rupture between stable angina and acute myocardial infarction: a three-vessel intravascular ultrasound study in 235 patients. *Circulation* 2004;110:928–33. <https://doi.org/10.1161/01.CIR.0000139858.69915.2E>
27. Chiorescu RM, Mocan M, Inceu AI, Buda AP, Blendea D, Vlaicu SI. Vulnerable atherosclerotic plaque: is there a molecular signature? *Int J Mol Sci* 2022;23:13638. <https://doi.org/10.3390/ijms232113638>
28. Vergallo R, Burzotta F, Aurigemma C, Romagnoli E, D'Amario D, Trani C, et al. The fingerprints of plaque rupture healing as detected by serial optical coherence tomography imaging. *EuroIntervention* 2022;18:e405–6. <https://doi.org/10.4244/EIJ-D-22-00007>
29. Shoji K, Wakana N, Zen K, Matoba S. Non-culprit ruptured vulnerable plaque healing and stabilization by an aggressive lipid-lowering therapy. *Int J Cardiovasc Imaging* 2021;37:1999–2000. <https://doi.org/10.1007/s10554-021-02198-z>
30. Hong MK, Mintz GS, Lee CW, Suh IW, Hwang ES, Jeong YH, et al. Serial intravascular ultrasound evidence of both plaque stabilization and lesion progression in patients with ruptured coronary plaques: effects of statin therapy on ruptured coronary plaque. *Atherosclerosis* 2007;191:107–14. <https://doi.org/10.1016/j.atherosclerosis.2006.02.040>
31. Vergallo R, Crea F. Atherosclerotic plaque healing. *N Engl J Med* 2020;383:846–57. <https://doi.org/10.1056/NEJMr2000317>
32. Otsuka F, Joner M, Prati F, Virmani R, Narula J. Clinical classification of plaque morphology in coronary disease. *Nat Rev Cardiol* 2014;11:379–89. <https://doi.org/10.1038/nrcardio.2014.62>
33. Libby P. Mechanisms of acute coronary syndromes and their implications for therapy. *N Engl J Med* 2013;368:2004–13. <https://doi.org/10.1056/NEJMr1216063>
34. Biccirè FG, Fabbicocchi F, Gatto L, La Manna A, Ozaki Y, Romagnoli E, et al. Long-term prognostic impact of OCT-derived high-risk plaque features: extended follow-up of the CLIMA study. *JACC Cardiovasc Interv* 2025;18:1361–72. <https://doi.org/10.1016/j.jcin.2025.04.044>
35. Xing L, Higuma T, Wang Z, Aguirre AD, Mizuno K, Takano M, et al. Clinical significance of lipid-rich plaque detected by optical coherence tomography: a 4-year follow-up study. *J Am Coll Cardiol* 2017;69:2502–13. <https://doi.org/10.1016/j.jacc.2017.03.556>
36. Cheruvu PK, Finn AV, Gardner C, Caplan J, Goldstein J, Stone GW, et al. Frequency and distribution of thin-cap fibroatheroma and ruptured plaques in human coronary arteries: a pathologic study. *J Am Coll Cardiol* 2007;50:940–9. <https://doi.org/10.1016/j.jacc.2007.04.086>
37. Araki M, Soeda T, Kim HO, Thondapu V, Russo M, Kurihara O, et al. Spatial distribution of vulnerable plaques: comprehensive in vivo coronary plaque mapping. *JACC Cardiovasc Imaging* 2020;13:1989–99. <https://doi.org/10.1016/j.jcmg.2020.01.013>
38. Stone GW, Maehara A, Lansky AJ, de Bruyne B, Cristea E, Mintz GS, et al. A prospective natural-history study of coronary atherosclerosis. *N Engl J Med* 2011;364:226–35. <https://doi.org/10.1056/NEJMoa1002358>
39. Taniwaki M, Radu MD, Garcia-Garcia HM, Heg D, Kelbaek H, Holmvang L, et al. Long-term safety and feasibility of three-vessel multimodality intravascular imaging in patients with ST-elevation myocardial infarction: the IBIS-4 (integrated biomarker and imaging study) substudy. *Int J Cardiovasc Imaging* 2015;31:915–26. <https://doi.org/10.1007/s10554-015-0631-0>